JOURNAL OF VIROLOGY, Mar. 1997, p. 2211–2216 Vol. 71, No. 3
0022-538X/97/$04.00+0

Two Proline Residues Are Essential in the Calcium-Binding Activity of Rotavirus VP7 Outer Capsid Protein

RODRIGO GAJARDO,† PATRICE VENDE, DIDIER PONCET, AND JEAN COHEN*

Laboratoire de Virologie et Immunologie Moléculaires, INRA, C.R.J., Domaine de Vilvert, 78350 Jouy-en-Josas, France

Received 12 August 1996/Accepted 11 December 1996

Rotavirus maturation and stability of the outer capsid are calcium-dependent processes. It has been shown previously that the concentration of Ca^{2+}-solubilizing outer capsid proteins from rotavirus particles is dependent on the virus strain. This property of viral particles has been associated with the gene coding for VP7 (gene 9). In this study the correlation between VP7 and resistance to low [Ca^{2+}] was confirmed by analyzing the origin of gene 9 from reassortant viruses prepared under the selective pressure of low [Ca^{2+}]. After chemical mutagenesis, we selected mutant viruses of the bovine strain RF that are more resistant to low [Ca^{2+}]. The genes coding for the VP7 proteins of these independent mutants have been sequenced. Sequence analysis confirmed that these mutants are independent and revealed that all mutant VP7 proteins have proline 75 changed to leucine and have an outer capsid that solubilized at low [Ca^{2+}]. The mutation of proline 279 to serine is found in all but two mutants. The phenotype of mutants having a single proline change can be distinguished from the phenotype of mutants having two proline changes. Sequence analysis showed that position 75 is in a region (amino acids 65 to 78) of great variability and that proline 75 is present in most of the bovine strains. In contrast, proline 279 is in a conserved region and is conserved in all the VP7 sequences in data banks. This region is rich in oxygenated residues that are correctly allocated in the metal-coordinating positions of the Ca^{2+}-binding EF-hand structure pattern, suggesting that this region is important in the Ca^{2+} binding of VP7.

Calcium is a ubiquitous intracellular signaling molecule controlling a wide range of cellular processes. The calcium concentration ([Ca^{2+}]) in a resting cell is maintained at approximately 10 to 100 nM. Outside the cell this concentration is several orders of magnitude higher (1 to 2 mM). During stimulation, the average intracellular [Ca^{2+}] can increase to several micromolar units. These [Ca^{2+}] changes can cause conformational modifications in many cell proteins such as calmodulin (25) and annexin V (7). It has also been documented that several viral infections, including human immunodeficiency virus type 1 (HIV-1) (5), cytomegalovirus (28), poliovirus (15), and rotavirus (27), involve increases of the intracellular [Ca^{2+}], suggesting that this ion plays an important role in the assembly and disassembly and/or replication processes. Many plant virus coat proteins have binding sites for divalent cations, particularly calcium (1, 10, 11, 19). It has been speculated that such sites ensure that plant viruses release their RNA only in the host cytoplasm, which has a low [Ca^{2+}]. Calcium appears also to be an integral part of the capsid proteins of several animal viruses, such as murine polyomavirus (22), simian virus 40 (21), influenza viruses (2), rotavirus (6, 35), HIV-1 (12), and nodavirus (37).

The rotavirus particle is nonenveloped and possesses a triple-layered capsid. The outer shell consists of major glycoprotein VP7 and VP4, a trypsin-sensitive protein forming dimers. The intermediate layer consists of VP6, the major capsid protein. The inner layer is formed by protein VP2 and minor proteins VP1 and VP3. Complete virions will be referred to as triple-layered particles (TLP) and viral particles without outer-layer proteins VP4 and VP7 will be referred to as double-layered particles (DLP).

Treatment of the rotavirus particles with chelating agents results in the removal of outer capsid proteins VP4 and VP7, leading to transcriptionally active DLP (6). Rotavirus morphogenesis is also dependent on the presence of Ca^{2+} in the culture medium. Culture medium without Ca^{2+} stops virus morphogenesis at the DLP step (35). Several lines of evidence support a specific role for VP7 in the Ca^{2+}-binding site. (i) In the absence of Ca^{2+}, VP7 is excluded from the hetero-oligomeric complex made of NSP4 and VP4 that participates in the budding of the DLP into the endoplasmic reticulum (23, 31). Furthermore, calcium depletion of the endoplasmic reticulum by thapsigargin inhibits VP7 and NSP4 glycosylation and virus maturation (26). (ii) Calcium chelation induces a conformational change in recombinant herpes simplex virus-expressed VP7, as measured by the loss of an epitope recognized by a monoclonal antibody (9). (iii) Genetic analysis of the [Ca^{2+}] needed to solubilize the outer capsid proteins in a set of reassortant viruses confirmed that this phenotype maps onto the gene coding for VP7 (34).

The calcium-binding site of VP7 is not yet localized even though a sequence analysis has made it possible to predict a putative site in group A rotavirus (amino acids [aa] 124 to 155) but not in groups B and C (24). To obtain information on this calcium-binding site, we selected mutant rotaviruses having their outer layer proteins solubilized at a lower [Ca^{2+}]. Sequencing gene 9 of these mutants allows the identification of two proline residues that are associated with the calcium-binding activity of rotavirus outer capsid protein.

MATERIALS AND METHODS

Cells and viruses. The following virus strains were used in this study. The RF (G6, P1) and UK (G6, P5) strains of bovine rotavirus; the simian strains SA11-4F (G3, P1), SA11-c13 (G3, P2), and RRV (G3, P3); the OSU strain (G5, P7) of porcine rotavirus; and the human strain Wa (G1, P8). All the viruses were

* Corresponding author. Phone: (331) 34 65 26 04. Fax: (331) 34 65 26 21. E-mail: cohen@biotec.jouy.inra.fr.

† Present address: Departament de Microbiologia, Facultat de Biologia, Universitat de Barcelona, 08028 Barcelona, Spain.

propagated in fetal rhesus monkey MA104 cells in the presence of trypsin (0.44 μg/ml; Sigma type IX). Strains SA11-4F and SA11-cl3 were kindly provided by M. K. Estes (Baylor College of Medicine, Houston, Tex.). Strain UK was kindly provided by D. Snodgrass (Moredun Research Institute, Edinburgh, Scotland, United Kingdom). When necessary, viruses were concentrated and purified by two runs of cesium chloride gradient after Freon 113 extraction. Virus titration was performed by plaque assay as previously described (30). Titers are expressed as PFU per milliliter.

Calcium buffers and virus treatment. Calcium buffers were prepared with Ca-EGTA and EGTA (10 mM) in 10 mM MOPS (morpholinepropanesulfonic acid) and 100 mM KCl and were adjusted to pH 7.2 with KOH, as described previously (36). Concentrated stocks of purified virus or cell-infected lysates were desalted by centrifugation through a Sephadex G-25 column equilibrated with 10 mM MOPS and 100 mM KCl and adjusted to pH 7.2 with KOH. Virus suspensions (1 volume) were mixed with 0.1 volume of 10× Ca^{2+} buffer and incubated for 15 min at room temperature. The reaction was stopped by adding 1 ml of minimal essential medium culture medium buffered with HEPES and supplemented with trypsin and by keeping tubes on ice until titration. The survival of the virus at different [Ca^{2+}] was determined by calculating the value of $\log_{10} N_{Ca}/N_i$, where N_i is the initial virus titer and N_{Ca} is the titer after treatment of the virus at a given [Ca^{2+}]. All the inactivation values reported are the averages of at least three separate experiments.

Generation of reassortant viruses under the selective pressure of low [Ca^{2+}]. SA11-c13 and RF viruses were used to perform mixed infections at a multiplicity of infection (MOI) of 5 PFU/cell for each parent. Unless otherwise indicated, all the infections were made in MA104 cells cultured in 25-cm^2 flasks. Aliquots of the reassortant progeny were propagated again at an MOI of about 10 PFU/cell. After three passages, one aliquot (100 μl) was treated with 100 nM free Ca^{2+} as described above and used to initiate serial passages. Another 100-μl aliquot was serial passaged without any selective pressure. After 10 cycles, 20 reassortant viruses were plaque purified from each passage series and analyzed for the origin of VP4 and VP7 proteins by reverse transcription-PCR (RT-PCR) with specific primers.

Reverse transcription was carried out with a pool of oligonucleotide primers containing RF-Beg9 (nucleotides 1 to 28) and RF-End9 (nucleotides 1062 to 1036) complementary to the 3′ ends of the negative and positive RNA strands, respectively, of the gene coding for the VP7 protein of the RF strain (accession number, X65940) and oligonucleotide primer VP4-5 complementary to the 3′ end (nucleotides 11 to 31) of the minus strand of the gene coding for protein VP4. Since the 5′ and 3′ ends of the VP4 and VP7 genes are well conserved (24), these primers allow the RT (and, eventually, the PCR amplification) of the VP4 genes from both the SA11-cl3 and RF strains. The origin of VP4 and VP7 was determined in a separate PCR with the same RT product. For VP4, oligonucleotide VP4-5 was used in combination with primers specific to SA11-cl3 (VP4-SA11, nucleotides 481 to 463 complementary to the plus strand; accession number, D16345) and to RF (primer VP4-RF, nucleotides 747 to 724 complementary to the plus strand; accession number, U65924). For VP7 determination, the primers RF-Beg9 and RF-End9 were used in combination with primers specific to SA11-cl3 (nucleotides 193 to 174 of SA11; accession number, VO1546) and RF (nucleotides 253 to 231 of RF). PCR of SA11 and RF gene 9 produced fragments 193 bp and 809 bp in length, respectively.

Mutagenesis. Two mutagens, 5-azacytidine (5-AC) and hydroxylamine (HA) (Sigma), were used essentially as previously described (32, 33) with minor modifications. Rotavirus strain RF was subjected to mutagenesis by multiplication in the presence of 5-AC. Cells were infected at an MOI of 10 PFU/cell and kept in medium containing 100 μg of 5-AC per ml. Virus was harvested at 24 to 36 h postinfection when complete cytopathic effect (CPE) was observed in the control infection in the absence of the mutagen. For HA mutagenesis, equal volumes of virus stock (RF strain; 10^8 PFU/ml) and 4 M HA prepared in 100 mM phosphate buffer (pH 6.0) were mixed and incubated for 40 min at room temperature. To remove HA, the mutagenized virus stocks were centrifuged through Sephadex G-25 spin columns equilibrated with phosphate-buffered saline buffer. Cell monolayers were infected with the mutagenized viral stocks to fix the mutation. Virus was collected when a clear CPE was detected. Inocula of mutated viruses were prepared from infected cultures subjected to three freeze-thaw cycles, and cell debris was removed by centrifugation at low speed. The low-[Ca^{2+}]-resistant mutants were selected from the resulting mutagenized stocks as described below.

Selection of low-[Ca^{2+}]-resistant mutants. To ensure that each mutant was independent of all other mutants, a single virus clone from one mutagenic reaction tube or culture flask was propagated. The mutant RF viruses resistant to low [Ca^{2+}] were selected by following two different strategies. The first strategy consisted of treating 100-μl aliquots of desalted mutagenized viral stocks (multiplied once in tissue culture) with 100 nM free Ca^{2+} as described above. Surviving viruses were plated and plaque purified. Agarose stab corresponding to individual plaque was incubated in MOPS buffer (10 mM MOPS and 100 mM KCl adjusted to pH 7.2 with KOH), and the eluted virus was treated again with 100 nM free Ca^{2+}. The treated virus was mixed with culture medium containing trypsin and inoculated into MA104 cells in 96-well plates. The medium in wells showing a clear CPE was collected. The corresponding virus was subjected to another selection by 100 nM free Ca^{2+} and amplified by infecting a MA104 monolayer in a 25-cm^2 culture flask. When the CPE was complete (2 to 3 days postinfection), cultures were subjected to three freeze-thaw cycles, and cell debris was removed by centrifugation. One hundred microliters of these lysates was desalted, treated with 100 nM free Ca^{2+}, and used to inoculate MA104 cells in a 25-cm^2 culture flask. Each viral clone was blind passaged 5 to 7 times, with a low [Ca^{2+}] selection (100 nM) between each passage, and was further plaque purified three times. The resulting viral clones were then assayed after treatment at various [Ca^{2+}].

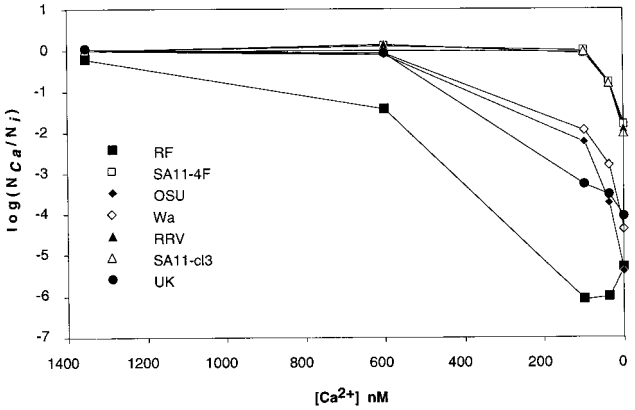

FIG. 1. Reduction of titer of several rotavirus strains as a function of the free [Ca^{2+}]. Crude lysates of infected cells were desalted and treated in 10 mM EGTA or Ca-EGTA buffers at various [Ca^{2+}], then titrated. The reduction of infectivity is expressed as $\log_{10} N_{Ca}/N_i$, where N_i is the initial virus titer and N_{Ca} is the titer after treatment of the virus at the given [Ca^{2+}]. The data are the averages of at least three separate experiments.

The second strategy to obtain mutant RF viruses was slightly different. After mutagenesis and fixation of the mutations, viruses were blind passaged and subjected to a treatment with 100 nM Ca^{2+} between each passage as described above. After 7 or 8 passages, viruses were plaque purified three times, amplified in cell culture, and characterized.

Electrophoresis. Electrophoresis of viral particles was performed as previously described (34) in 0.6% agarose gel in 10 mM MOPS-Tris (pH 7.1) buffer for 2 h at 80 V. Gels were stained with silver complexes by using the Bio-Rad Silver Stain Plus kit.

Sequencing of the low-[Ca^{2+}]-resistant mutants and parental virus. Sequence determination of gene segment 9, coding for VP7 protein, of the RF parental strain and mutants was by direct sequencing of PCR-amplified DNA. Full-length cDNA was generated with viral RNA extracted from infected cell supernatants in a combined RT-PCR amplification carried out with oligonucleotide primers specific for gene 9 (RF-Beg9 and RF-End9) and complementary to the 3′ ends of both viral RNA strands. Both DNA strands were sequenced with eight different primers (four primers/strand) and the *Taq* Dye Terminator Cycle Sequencing kit of Perkin-Elmer. It should be noted that this strategy did not make it possible to determine the 10 to 15 nucleotides at the 5′ and 3′ ends of the gene. However, it has been shown that these regions are noncoding regions and that little or no sequence variation is present within group A rotaviruses (13). Sequence analysis was performed with the Genetics Computer Group package (8).

RESULTS

Inactivation of various rotavirus strains by low [Ca^{2+}]. It was previously shown (34) that the concentration of Ca^{2+} needed to solubilize the outer capsid proteins of rotavirus particles, as estimated by gel electrophoresis and light scattering, varies with the strain. During this work, another procedure to evaluate the solubilization process of outer proteins at various free [Ca^{2+}] was designed. It is based on the fact that solubilization of the outer layer induces a loss of infectivity that can be measured by simple plaque assay. The reduction in titer of several rotavirus strains after a 15-min treatment at defined free [Ca^{2+}] ranging from 0 to 1000 nM is shown in Fig. 1. Bovine strain RF was the most susceptible strain, showing greater titer reductions ($\log_{10} N_{Ca}/N_i$) than the other tested strains. For this strain, at 600 nM free Ca^{2+} a titer reduction of 1.41 was found, whereas at 100 nM the reduction was 6.1. We considered this titer reduction the residual titer reduction since reducing the [Ca^{2+}] to zero did not induce any further de-

TABLE 1. RF and SA11-cl3 reassortant selection is correlated with the presence of the SA11-cl3 VP7 protein

Selective pressure[a]	No. of clones having the gene for:			
	VP7 from SA11-cl3	VP7 from RF	VP4 from SA11-cl3	VP4 from RF
Without	8	12	0	20
With	20	0	0	20

[a] Selective pressure consisted of treatment with 100 nM Ca^{2+} between each passage. Total number of clones, 20.

crease. The simian strains (SA11-4F, SA11-cl3, and RRV) were found to be the most resistant strains, showing no titer reduction at [Ca^{2+}] equal to or above 100 nM free Ca^{2+}. For these simian strains the reduction of titer after treatment at 38 nM free Ca^{2+} was around 0.8. Strains OSU and Wa displayed intermediate behavior, with titer reductions of 2.24 and 1.94, respectively, at 100 nM free Ca^{2+} and 3.74 and 2.8, respectively, at 38 nM free Ca^{2+}. Bovine strain UK showed a titer reduction of 3.26 and 3.87 after treatment at 100 and 38 nM free Ca^{2+}, respectively. This result was unexpected because the UK and RF strains have very similar VP7 (seven amino acid substitutions; Fig. 4).

VP7 from SA11 is positively selected after coinfection (SA11-cl23×RF) and selection at low [Ca^{2+}]. Several studies have shown the involvement of VP7 in rotavirus low-[Ca^{2+}]-mediated outer capsid solubilization. The aim of this experiment was to demonstrate that selection at low [Ca^{2+}] of reassortant populations resulting from the coinfection of two rotavirus strains of different phenotypes (SA11-cl3 and RF) would lead to viruses having the VP7 from the strain more resistant to solubilization by low [Ca^{2+}]. The results shown in Table 1 demonstrate that VP7 from SA11-cl3 is positively selected after 10 passages under the selective pressure of 100 nM Ca^{2+}. In the control experiment, in the absence of selective pressure, 40% of the population was found to have the VP7 from SA11-cl3 and 60% the VP7 from RF. All the resulting reassortant viruses, selected or not by low [Ca^{2+}], were found to possess VP4 from RF (Table 1). The unexpected segregation of the gene coding for this protein precluded us from elucidating the role of low [Ca^{2+}] on VP4.

Titration of these reassortant viruses after treatment at various [Ca^{2+}] showed a perfect correlation between the origin of the VP7 and the inactivation rate at low [Ca^{2+}] (data not shown).

Mutagenesis and selection of low [Ca^{2+}]-resistant mutants. In order to determine the region(s) of the VP7 protein involved in the low-[Ca^{2+}]-mediated solubilization of the outer capsid, we selected mutants of the RF strain whose infectivity is not affected by low [Ca^{2+}]. First we tried to isolate naturally occurring mutant RF viruses. Purified virus stocks containing 10^{11} to 10^{12} PFU/ml were incubated in calcium-free buffer (2 mM EGTA) and plated, and recovered plaques were tested for resistance to treatment by various [Ca^{2+}]. All the 200 recovered viral clones were found to have the parental behavior (data not shown), indicating that the surviving viruses were not mutants, but rather corresponded to the residual titer. Conditions of mutagenesis with HA and 5-AC that induce frequent mutations, while avoiding the induction of multiple mutations, were derived from the construction of rotavirus temperature-sensitive mutants of the SA11 strain (32, 33). These mutagenesis levels corresponded to a surviving fraction, after treatment with HA and 5-AC, of approximately 0.3 and 0.1, respectively. From these mutagenenized stocks, seven independent mutants were isolated. Following HA mutagenesis and the first selection procedure (as described in Materials and Methods), 546 plaques were screened and three independent mutants were isolated (m114, m150, and m748). One mutant (m502) was isolated from the 328 plaques screened following 5-AC mutagenesis. By using the second selection procedure and after mutagenesis with HA and 5-AC, one (mH2) and two mutants (mA5 and mA6), respectively, were isolated.

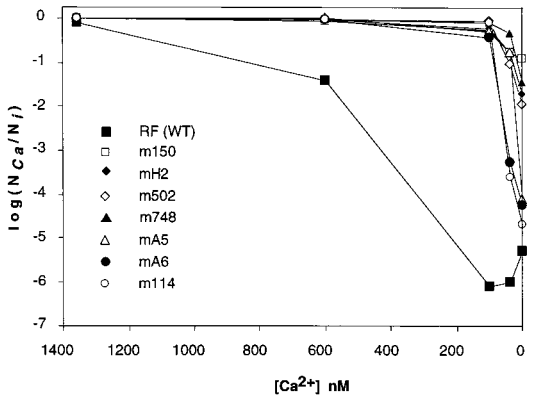

FIG. 2. Reduction of titer of RF mutants as a function of the free [Ca^{2+}]. Crude lysates of cells infected with the mutant viruses were titrated on MA104 monolayers after treatment with various [Ca^{2+}]. Reductions of viral titers were calculated as indicated in Materials and Methods. The data for the wild-type RF virus (derived from Fig. 1) are shown for comparison. These results are the averages of at least three separate experiments.

Characterization of RF mutant viruses at low [Ca^{2+}]. The above-mentioned mutants were characterized for survival at various free [Ca^{2+}]. As shown in Fig. 2, no significant decrease in titer was detected after treatment of all mutants with 600 nM Ca^{2+}. For parental strain RF, the reduction of titer ($\log_{10} N_{Ca}/N_i$) was 1.86. At 100 nM Ca^{2+} the reductions in titer of the mutants ranged between 0.1 (m748) and 0.45 (mA6), showing no significant variation between mutants. In contrast, two groups of mutants could be defined according to the inactivation rate at 38 nM free Ca^{2+}. One group consists of the mutants m114 and mA6, which showed a reduction in titer of 3.6 and 3.27, respectively. The second group consists of the other five mutants, which showed titer reductions ranging from 0.34 (m748) to 1.04 (m502) at the same [Ca^{2+}].

To confirm that this inactivation was due to the solubilization of the outer capsid proteins, the TLP-to-DLP transition was analyzed by electrophoresis in agarose gel after incubating wild-type RF and mutants at various [Ca^{2+}]. Transition of wild-type RF virus started at a [Ca^{2+}] of about 1,000 nM, and the complete conversion into DLP was at 600 nM (Fig. 3A). The reduction in titer measured in the same experiment (Fig. 3B) confirmed the agreement between the TLP-to-DLP transition and the reduction in infectivity. Two mutant viruses (mA6 and m748) were chosen as representative of the abovementioned two groups of mutants. For both mutants (Fig. 3), TLP-to-DLP transition began at a [Ca^{2+}] of 100 nM and complete conversion into DLP was at 17 nM. However, slight differences between the mutants could be reproducibly observed at 38 nM free Ca^{2+} (Fig. 3A). For mutant mA6, most of the particles were converted to DLP, whereas for mutant m748 most of the particles migrated in a very diffuse band above the band of DLP. This difference is consistent with the reductions in titer during this experiment, which were 1.38 and 0.38 for mA6 and m748, respectively (Fig. 3B). This difference in titer reductions was also observed after incubation of both mutants at 17 nM free Ca^{2+}.

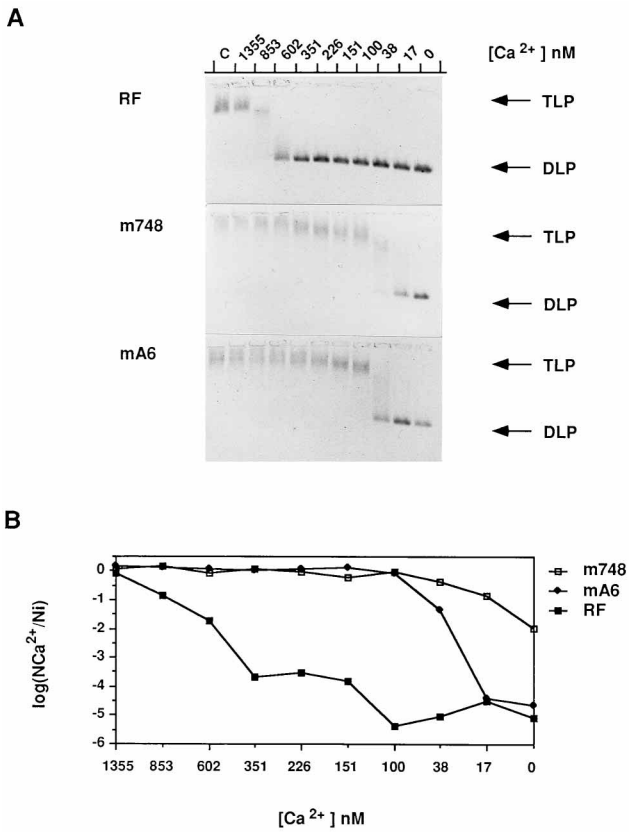

FIG. 3. Phenotype analysis of wild-type and mutant RF viruses. Purified TLP from the wild-type RF strain and from two representative mutant viruses having the Pro_{75}→Leu and the Pro_{279}→Ser or only the Pro_{75}→Leu (m748 and mA6, respectively) were treated with EGTA or Ca-EGTA buffer at various [Ca^{2+}]. After a 15-min treatment, samples were placed on ice and divided in two. One half was loaded onto an agarose gel (A). The other half was diluted with culture medium, and the titers were determined by plaque assay. The reductions of viral titer, calculated as indicated in Materials and Methods, are shown in panel B. This experiment was performed three times with similar results. The result of a single experiment is shown.

The phenotypes of all the mutants were stable after five passages under nonselective conditions (data not shown). Viral yields, plaque sizes, and times to produce CPE were not different between mutant and wild-type viruses.

Mutations within the VP7 deduced amino acid sequences of the selected mutants. The sequence of gene 9 of the RF strain coding for VP7 was previously published (3). To detect sequence variation after several passages, the virus stock used in the present work was sequenced again. We refer to this last sequence as the wild-type sequence. It presents, with respect to the published sequence, two deduced amino acid substitutions, lysine to asparagine at position 49 (Lys_{49}→Asn) and Leu_{317}→Phe and a base change in the 5′ noncoding region. All the base changes and deduced amino acid substitutions found in the low [Ca^{2+}] mutants are shown in Table 2. All the mutants have in common the substitution Pro_{75}→Leu. All but two (mA6 and m114) have also the change Pro_{279}→Ser. Note that the presence of single mutations confirmed that each mutant virus was independently obtained.

Thus, a single proline-to-leucine substitution at position 75 of VP7 was sufficient to vary the [Ca^{2+}] needed to stabilize the outer capsid proteins in strain RF. The additional change Pro_{279}→Ser resulted in greater stability at low [Ca^{2+}].

Except for the proline substitutions, the silent base changes, and the mutations within the noncoding regions, two mutants were found to present amino acid substitutions. Mutant mA6 had the change Val_{303}→Ile and mutant m502 had the change Thr_{27}→Ser within the region considered the signal peptide. Both these substitutions can be considered conservative.

TABLE 2. Mutations in the gene coding for VP7 of the RF mutants resistant to low [Ca^{2+}] and deduced amino acid changes

Mutant	Base positions	Base changes	aa substitutions
m748	272	C→T	Pro_{75}→Leu
	883	C→T	Pro_{279}→Ser
m502	127	A→T	Thr_{27}→Ser
	272	C→T	Pro_{75}→Leu
	883	C→T	Pro_{279}→Ser
mA5	28	G→C	Noncoding region
	272	C→T	Pro_{75}→Leu
	883	C→T	Pro_{279}→Ser
m150	198	G→C	None
	272	C→T	Pro_{75}→Leu
	883	C→T	Pro_{279}→Ser
mH2	115	T→C	None
	117	A→C	None
	272	C→T	Pro_{75}→Leu
	883	C→T	Pro_{279}→Ser
m114	272	C→T	Pro_{75}→Leu
	699	A→G	None
mA6	272	C→T	Pro_{75}→Leu
	955	G→A	Val_{303}→Ile

DISCUSSION

We confirmed that various rotavirus strains had different resistances to low [Ca^{2+}]. The production of reassortant viruses showed that this phenotype was correlated with the product of gene 9. This experiment failed to elucidate the role of VP4, since VP4 from RF was selected either with or without selective pressure. The nonrandom segregation of gene 4 has been previously described (38) and suggests that the VP4 from RF provides a replication advantage independently of the VP7 origin. It has also been shown that VP4 can affect the conformation of VP7 (4). Thus, although VP7 is considered the main protein responsible for the solubilization of both proteins at low [Ca^{2+}], the origin of VP4 could modify the [Ca^{2+}] needed to solubilize the outer capsid. Considering the results published by Ruiz et al. (34) and the results described here, the VP4 influence is necessarily minor.

Using Ca-EGTA buffer, we developed a strategy to recover seven independent mutant viruses that survived after low [Ca^{2+}] treatment. All these mutants had a change of proline to leucine at position 75, and five of the mutants showed an extra change of proline to serine at position 279, demonstrating that these two residues are very important in the Ca^{2+} binding of VP7.

Amino acid substitutions found in the low-[Ca^{2+}]-resistant mutants pointed to two regions of VP7. The change in the region under the influence of Pro-75 can be considered the most important since this single substitution (present in mutants mA6 and m114) is responsible for the phenotype at low [Ca^{2+}]. The additional change Pro_{279}→Ser never occurred alone, suggesting that this second mutation was dependent on

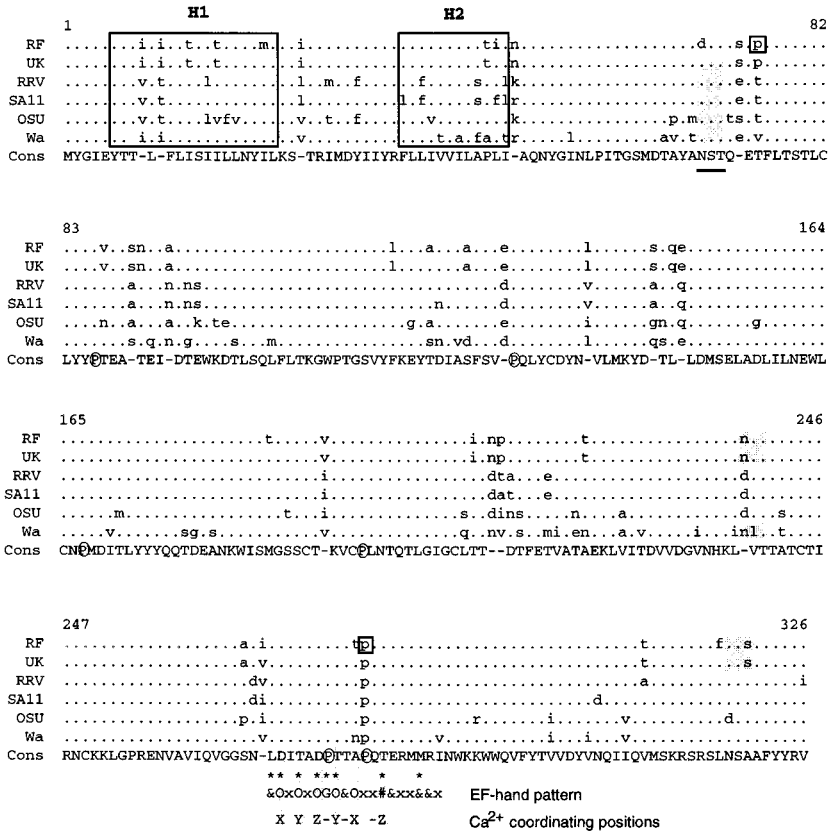

FIG. 4. Sequence alignment of VP7 sequences from the strains used in this study. Boxed prolines in RF are the mutated prolines in the low-[Ca^{2+}]-resistant mutants. Proline residues conserved in all group A rotaviruses are circled. Signal peptides H1 and H2 are boxed. Potential glycosylation sites are shaded, and the proven glycosylation site in SA11 is underlined. In the region of the Pro_{279}→Ser mutation, the EF-hand pattern is shown below the consensus sequence. In this pattern, the following symbols are used: &, hydrophobic residue; O, oxygen-containing residue; §, negatively charged residue; #, negatively charged or oxygen-containing residue; x, any amino acid. Asterisks indicate the residues of VP7 that match the EF-hand pattern (8 of 12 defined positions). X, Y, Z, −Y, −X, and −Z indicate residues that directly coordinate Ca^{2+} in the EF-hand structure and refer to the vertices of the Ca^{2+} coordination octahedron.

the Pro_{75}→Leu change. This second change resulted in greater stability at low [Ca^{2+}].

Sequences of VP7 from the strains used in this work were compared to each other (Fig. 4) and also to all group A VP7 sequences present in data banks (data not shown). Pro-75 is only present in bovine strains RF and UK; in strains RRV, SA11, and OSU this position is occupied by Thr, and in strain Wa it is occupied by Val. Position 75 is included in a region (residues 65 to 78) of high variability. Among the available VP7 sequences there is a series of residues (I, M, N, P, S, T, V) at position 75, but none of these sequences has a Leu as do all the mutants isolated here. Note that most of the bovine strains have a Pro at residue 75. Pro-75 is four residues down a glycosylation site that is conserved in all the virus strains used here except the RF strain.

Although they have very similar VP7s, strains RF and UK have different behavior at low [Ca^{2+}], as estimated by the infectivity decrease. The main difference between the proteins is a glycosylation site at position 69 in UK and not in RF. This fact points out how important the region of Pro-75 could be in Ca^{2+}-dependent stability. It has been previously shown that glycosylation can affect the conformation of VP7 (20), and changes in this region can stabilize or destabilize the Ca^{2+}-binding site by bringing closer or pushing away the residues involved at the site.

In contrast to the variability of Pro-75, Pro-279, which is in a conserved region, is present in all the strains used in this study and in all the VP7 sequences available in data banks. The very close Pro-275 is also conserved in all the available sequences.

Although Ca^{2+}-binding sites in several cellular Ca^{2+}-binding proteins have been extensively studied and well described by the helix-loop-helix EF-hand structure (for a review see reference 17), little is known about the nature of the Ca^{2+}-binding sites present in viral proteins. Similarities between the EF-hand structure and sequences present in viral proteins have been proposed (12, 14), but it can be considered that there is no archetypal viral Ca^{2+}-binding site. Ca^{2+}-binding sites in viral proteins are diverse in their coordination numbers and geometries. Viral Ca^{2+}-binding sites are in some cases shared by two capsid proteins, the Ca^{2+} forming a bridge that links two different capsid monomers (21, 37). A Ca^{2+}-binding site is formed by amino acids that directly coordinate Ca^{2+} with the side chain or backbone carbonyl oxygen (39) and by amino acids that do not coordinate Ca^{2+} directly but are important in maintaining the configuration of the site. The residues that are structurally relevant were identified by protein crystallization and X-ray diffraction (1, 16, 21, 29). The use of reverse genetics to produce mutants in putative Ca^{2+}-binding domains of viral proteins has also been helpful for determining the altered functions (14, 19).

The region of Pro-279 is rich in oxygenated residues. Some residues are at positions that correspond to metal-coordinating positions in the EF-hand structure (X, Y, Z, −Y, −X, −Z). In

addition, 8 of 12 putative EF-hand positions harbored canonical residues (Fig. 4). The substitution of glycine by proline at position 8 could also be important, but both residues are α-helix breakers and the change is considered conservative. At position −Z, the consensus is an acidic residue, but in many characterized EF-hand structures there is an amino acid with an oxygen atom on the side chain (12, 18). Although proline residues never occur in Ca^{2+}-coordinating positions in the EF-hand structure, in the influenza B neuraminidase, a proline coordinates Ca^{2+} throughout a water molecule (2). The similarity shown between the EF-hand structure and the region of Pro-279 does not prove that this region is the actual Ca^{2+}-binding region. However, it suggests that this region could be important in keeping the functional conformation of VP7 and that it plays a role in Ca^{2+} binding.

This sequence analysis, based on the importance of Pro-75 and Pro-279, is not consistent with the prediction of a Ca^{2+}-binding site between aa 124 and 155 (24). Note also that the reported binding site (aa 94) of neutralizing monoclonal antibody 159, whose interaction with VP7 is sensitive to $[Ca^{2+}]$, is not close to the regions identified here (9). The Ca^{2+}-binding site could consist of residues dispersed along the primary structure of the protein. A comparison of the sequences of the various VP7 proteins also suggests that other residues could be implicated in the Ca^{2+}-binding site. For example both SA11 and OSU viruses have Thr-75 and Pro-279 but SA11 is more stable than OSU (34). Most of the Ca^{2+}-binding sites in viral proteins already identified are noncontinuous. They have most of the coordinating residues close together and a few further away in the linear molecule (1, 2, 16, 21, 29).

Data presented here indicate that the Ca^{2+}-binding site in VP7 involves two distant regions that could be close together in the folded molecule. More work is needed to determine if the regions interacting belong to the same VP7 molecule.

ACKNOWLEDGMENTS

R. Gajardo is funded in part by a fellowship from Formación de Personal Investigador en el Extranjero from the Ministerio de Educación y Cienca (Spain).

We kindly acknowledge A. Benmansour for helpful discussions, A. Charpilienne for her efficient technical help, and C. Young for revising the English.

REFERENCES

1. **Abdel-Meguid, S., S. T. Yamane, K. Fukuyama, and M. G. Rossmann.** 1981. The location of calcium ions in southern bean mosaic virus. Virology **114:** 81–85.
2. **Burmeister, W. P., R. W. Ruigrok, and S. Cusack.** 1992. The 2.2 A resolution crystal structure of influenza B neuraminidase and its complex with sialic acid. EMBO J. **11:**49–56.
3. **Charpilienne, A., F. Borras, L. D'Auriol, F. Galibert, and J. Cohen.** 1986. Sequence of the gene encoding the outer glycoprotein of the bovine rotavirus (RF strain) and comparison with homologous genes from four bovine, simian and human rotaviruses. Ann. Inst. Pasteur (Virol.). **137:**71–77.
4. **Chen, D. Y., M. K. Estes, and R. F. Ramig.** 1992. Specific interactions between rotavirus outer capsid proteins VP4 and VP7 determine expression of a cross-reactive, neutralizing VP4-specific epitope. J. Virol. **66:**432–439.
5. **Cloyd, M. W., W. S. Lynn, K. Ramsey, and S. Baron.** 1989. Inhibition of human immunodeficiency virus (HIV-1) infection by diphenylhydantoin (dilantin) implicates role of cellular calcium in virus life cycle. Virology **173:** 581–590.
6. **Cohen, J., J. Laporte, A. Charpilienne, and R. Scherrer.** 1979. Activation of rotavirus RNA polymerase by calcium chelation. Arch. Virol. **60:**177–186.
7. **Concha, N. O., J. F. Head, M. A. Kaetzel, J. R. Dedman, and B. A. Seaton.** 1993. Rat annexin V crystal structure: Ca(2+)-induced conformational changes. Science **261:**1321–1324.
8. **Devereux, J., P. Haeberli, and O. Smithies.** 1984. A comprehensive set of sequence analysis programs for the VAX. Nucleic Acids Res. **12:**387–395.
9. **Dormitzer, P. R., and H. B. Greenberg.** 1992. Calcium chelation induces a conformational change in recombinant herpes simplex virus-1-expressed rotavirus VP7. Virology **189:**828–832.
10. **Durham, A. C., and D. A. Hendry.** 1977. Cation binding by tobacco mosaic virus. Virology **77:**510–519.
11. **Durham, A. C. H., and M. A. Haidar.** 1977. Cation binding by tobacco rattle virus. Virology **77:**520–523.
12. **Ebenbichler, C. F., H. Stoiber, R. Schneider, J. R. Patsch, and P. Dierich.** 1996. The human immunodeficiency virus type 1 transmembrane gp41 protein is a calcium-binding protein and interacts with the putative second-receptor molecules in a calcium-dependent manner. J. Virol. **70:**1723–1728.
13. **Estes, M. K., and J. Cohen.** 1989. Rotavirus gene structure and function. Microbiol. Rev. **53:**410–449.
14. **Haynes, J. I., D. Chang, and R. A. Consigli.** 1993. Mutations in the putative calcium-binding domain of polyomavirus VP1 affect capsid assembly. J. Virol. **67:**2486–2495.
15. **Irurzun, A., J. Arroyo, A. Alvarez, and L. Carrasco.** 1995. Enhanced intracellular calcium concentration during poliovirus infection. J. Virol. **69:**5142–5146.
16. **Jones, T. A., and L. Liljas.** 1984. Structure of satellite tobacco necrosis virus after crystallographic refinement at 2.5 A resolution. J. Mol. Biol. **177:**735–767.
17. **Kawasaki, H., and R. H. Kretsinger.** 1994. Calcium-binding proteins. 1: EF-hands. Protein Profile **1:**343–349.
18. **Kretsinger, R., H. D. Tolbert, S. Nakayama, and W. Pearson.** 1991. The EF-hand, homologs and analogs, p. 17–38. *In* C. Heizmann (ed.), Novel calcium binding proteins: fundamentals and clinical implications. Springer-Verlag, Berlin, Germany.
19. **Laakso, M. M., and L. A. Heaton.** 1993. Asp→Asn substitutions in the putative calcium-binding site of the turnip crinkle virus coat protein affect virus movement in plants. Virology **197:**774–777.
20. **Lazdins, I., B. S. Coulson, C. Kirkwood, M. Dyall-Smith, P. J. Masendycz, S. Sonza, and I. H. Holmes.** 1995. Rotavirus antigenicity is affected by the genetic context and glycosylation of VP7. Virology **209:**80–89.
21. **Liddington, R. C., Y. Yan, J. Moulai, R. Sahli, T. L. Benjamin, and S. C. Harrison.** 1991. Structure of simian virus 40 at 3.8-A resolution. Nature **354:**278–284.
22. **Ludlow, J. W., and R. A. Consigli.** 1987. Localization of calcium on the polyomavirus VP1 capsid protein. J. Virol. **61:**2934–2937.
23. **Maass, D. R., and P. H. Atkinson.** 1990. Rotavirus proteins VP7, NS28, and VP4 form oligomeric structures. J. Virol. **64:**2632–2641.
24. **Mattion, N. M., J. Cohen, and M. K. Estes.** 1994. Rotavirus proteins, p. 169–249. *In* A. Kapikian (ed.), Viral infections of the gastrointestinal tract. Marcel Dekker, Inc., New York, N.Y.
25. **McPhalen, C. A., N. C. Strynadka, and M. N. G. James.** 1991. Calcium-binding sites in proteins: a structural perspective. Adv. Protein Chem. **42:** 77–144.
26. **Michelangeli, F., F. Liprandi, M. E. Chemello, M. Ciarlet, and M. C. Ruiz.** 1995. Selective depletion of stored calcium by thapsigargin blocks rotavirus maturation but not the cytopathic effect. J. Virol. **69:**3838–3847.
27. **Michelangeli, F., M. C. Ruiz, J. R. del Castillo, J. E. Ludert, and F. Liprandi.** 1991. Effect of rotavirus infection on intracellular calcium homeostasis in cultured cells. Virology **181:**520–527.
28. **Nokta, M., D. Eaton, O. S. Steinsland, and T. Albrecht.** 1987. Ca2+ responses in cytomegalovirus-infected fibroblasts of human origin. Virology **157:**259–267.
29. **Pattanayek, R., and G. Stubbs.** 1992. Structure of the U2 strain of tobacco mosaic virus refined at 3.5 A resolution using X-ray fiber diffraction. J. Mol. Biol. **228:**516–528.
30. **Poncet, D., G. Corthier, A. Charpilienne, and J. Cohen.** 1990. A recombinant vaccinia virus expressing the major capsid protein of simian rotavirus-induced anti-rotavirus antibodies. Virus Res. **15:**267–274.
31. **Poruchynsky, M. S., D. R. Maas, and P. H. Atkinson.** 1991. Calcium depletion blocks the maturation of rotavirus by altering the oligomerization of virus-encoded proteins in the ER. J. Cell Biol. **114:**651–661.
32. **Ramig, R. F.** 1982. Isolation and genetic characterization of temperature-sensitive mutants of simian rotavirus SA11. Virology **120:**93–105.
33. **Ramig, R. F.** 1983. Isolation and genetic characterization of temperature-sensitive mutants that define five additional recombination groups in simian rotavirus SA11. Virology **130:**464–473.
34. **Ruiz, M. C., A. Charpilienne, F. Liprandi, R. Gajardo, F. Michelangeli, and J. Cohen.** 1996. Concentration of Ca2+ that solubilizes outer capsid proteins from rotavirus particles is dependent on the strain. J. Virol. **70:**4877–4883.
35. **Shahrabadi, M. S., and P. W. Lee.** 1986. Bovine rotavirus maturation is a calcium-dependent process. Virology **152:**298–307.
36. **Tsien, R., and T. Pozzan.** 1989. Measurement of cytosolic free Ca2+ with Quin2. Methods Enzymol. **172:**230–263.
37. **Wery, J. P., V. S. Reddy, M. V. Hosur, and J. E. Johnson.** 1994. The refined three-dimensional structure of an insect virus at 2.8 A resolution. J. Mol. Biol. **235:**565–586.
38. **Xu, Z., and G. N. Woode.** 1994. Studies on the influence of the VP7 gene on rotavirus replication. Virology **198:**394–398.
39. **Yamashita, M. M., L. Wesson, G. Eisenman, and D. Eisenberg.** 1990. Where metal ions bind in proteins. Proc. Natl. Acad. Sci. USA **87:**5648–5652.